J. Surface Sci. Technol., Vol 22, No. 3-4, pp. 177-194, 2007

Isotropic to Nematic Phase Transition in F-actin

N. CHAKRABARTI* and P. DAS**
Department of Chemistry, Bose Institute, 93/1 A. P. C. Road, Calcutta 700 009, India

Abstract — Like a few other rod-like and semi-rigid polyelectrolytes, filamentous actin (F-actin) shows, respectively, an isotropic to nematic (I-N) phase transition and an aggregation to a hexagonal liquid crystal followed by paracrystals at low and moderately high salt concentrations. Its polyion characteristics, e.g., large bare diameter, imposing chain length, high molecular weight per unit chain contour length and large electronic charge spacing along the chain contour, make it stand out among the members of the family of rigid and semi-rigid lyotropic mesogens. The first-order I-N phase separation has been explored, at the level of the second virial approximation, for a rod-like model of the actin filament in a solution containing simple electrolytes such as KCl and $MgCl_2$. The calculation of concentrations in the coexisting isotropic and anisotropic (nematic) phases, and of the order parameter in the anisotropic phase has been attempted by following the approach of Stroobants et al. which takes account the repulsive but not the attractive interactions. A criterion for the stability of the isotropic phase, according to Odijk, considers the second and the third virial coefficients, and has been employed to describe the I-N phase diagram depicting filament length versus actin concentration. The nature of the I-N phase transition, which has both first-order and higher-order (continuous) parts, has been discussed.

Keywords : *F-actin, isotropic phase, nematic phase, liquid crystal, paracrystals.*

INTRODUCTION

Filamentous actin (F-actin) is a protein polymer occurring in muscle and non-muscle cells of the eukaryotic type [1]. These filaments have important roles in the maintenance of cellular shapes and motility. Each filament is formed by a concatenation of globular G-actin protein molecules. The polymerization process is typically initiated by a salt solution comprised of 100 mM KCl and 2 mM

*Present Address : Department of Physics, Bangabasi College, 19 Rajkumar Chakraborty Sarani, Kolkata-700 009. Email : pdas@bosemain.boseinst.ac.in; Fax : 91-33-2350 6790
**Author for correspondance.

$MgCl_2$, the pH being maintained at about 7.0 with imidazole-HCl or tris-HCl buffer. The uncontrolled polymerization leads to a very wide length distribution of actin filaments. However, in the presence of gelsolin (a capping protein) the filament length distribution is quite sharp [2].

Like other rodlike or semi-rigid polymer molecules, e.g., Tobacco Mosaic Virus (TMV) [3], F-actin solution exhibits an isotropic-nematic phase separation above a (low) threshold concentration [2]. This observation has been rationalized with the statistical mechanical theory of rigid rods, due to Onsager (1949) [4, 5, 6], who attributed the appearance of a nematic phase to a balance between steric pair interaction and the force due to the rotational thermal motion. The nematic phase appeared at a low concentration due to the imposing length of the polymers, and hence the probability of ternary and higher collisions is low. Thus, in the cluster or virial expansion of the free energy only up to the second term is retained. This is the so-called second virial approximation.

However, cylindrical rodlike polyelectrolytes in solution repel each other electrostatically. In the presence of added salts like KCl and $MgCl_2$ (as in the case of F-actin), the coulombic repulsion is screened. The interaction between a pair of long charged parallel and skew cylinders can both be estimated from a solution of the linear Poisson-Boltzmann equation under conditions of low salt concentration (~ 0.1 M KCl) and low surface potential (25 mV or thereabouts). The Onsager model [4] has been extended by Stroobants et al. [7, 8] to include cases in which interacting colloid particles have electric double layers. These authors showed that the isotropic-nematic transition cannot be described solely in terms of an effective diameter, and that the twisting effect has to be taken into account. The twisting effect serves to destabilize the liquid crystalline phase, moving it to higher concentrations. However, in general, the stabilizing influence due to effective (rod) diameter enhancement is supposed to dominate any destabilization due to twisting [7].

Proteins are a very important class of biocolloid, amphiphilic in nature containing considerable hydrophobic parts [9]. Hence protein-protein interaction should include an attraction which occurs between hydrophobic surfaces [10]. This long-range interaction has been attributed to weak long range, irrespective of the chemical nature of the surface. Van der Waals attraction is rather short-range, and especially important in describing coagulation of colloids, which is due to the primary minimum in the potential energy versus inter-particle separation curve [11].

The long-range attraction is strong enough to enforce stability of a hexagonal phase at low ionic strength. This has been observed to be the case for TMV [12] as well as for F-actin [13]. Binary collisions between polyions are unaffected by long-range attractive forces whereas the impact on ternary collisions is enormous.

These ideas have been used to derive a stability criterion for the isotropic phase by Odijk [12], using the second and the third virial coefficients. The isotropic phase becomes unstable with respect to isotropic-nematic phase separation, aggregation to hexagonal LC phase, etc., when the third virial coefficient becomes sufficiently negative due to the presence of long-range attractive forces.

The main purpose of this work is to discuss the isotropic-nematic phase transition in F-actin solution, as a function of filament length and ionic strength of the solution. When the average filament length, $L = 2$ mm, the phase transition is first-order [14], and the approaches of Onsager and Stroobant et al. [4,7] may be applicable in estimating coexisting concentrations and order parameter. However, I-N transition in F-actin becomes apparently continuous for longer filaments. Theoretical arguments based on the phenomenological Landau-deGennes approach categorize the I-N transition as weakly first-order [5]. A hexagonal LC phase [13] and bundling or paracrystals [15] are observed at moderately higher ionic strengths. An attempt has been made to rationalize these observations and explain the I-N phase diagram showing filament length (μm) versus actin concentration (mg/ml) in terms of the stability criterion alluded to above.

With the above introduction, we shall present summaries of the extension of Onsager approach by Stroobant et al. followed by the stability criterion proposed by Odijk. Finally, we shall present the results and the relevant discussion with a conclusion.

I-N Phase Separation in Rodlike Polyelectrolyte : *Repulsions Only* — The theoretical treatments considered in this work are restricted to monodisperse (i.e., all polymer molecules have identical lengths) systems. Above a critical concentration, solutions of rod-like particles undergo a phase separation into an isotropic phase and an anisotropic phase, coexisting in equilibrium. In the latter phase the particles have a preferred orientation. In the presence of excess electrolyte, the electrostatic repulsion between the rod-like particles influences strongly the formation of the anisotropic liquid crystal phase. Onsager [4] already indicated that the effect of electrostatic repulsion will be equivalent to an increase of the effective diameter. This effective diameter (D_{eff}) will be dependent on the thickness of the electric double layer and thus on the ionic strength. However, the electrostatic repulsion also depends on orientation and thus the effect of the electrostatic repulsion will be different in the isotropic phase from that in the anisotropic phase. The expression for the Helmholtz free energy proposed by Onsager can be modified including electrostatic repulsion with excluded volume interaction as [7]

$$\frac{\Delta F}{Nk_BT} = \frac{F(\text{solution}) - F(\text{solvent})}{Nk_BT}$$

$$= \frac{\mu^0(T,\mu_0)}{k_BT} - 1 + \ln c + \int d\mathbf{u}\, f(\mathbf{u}) \ln(4\pi f(\mathbf{u})) +$$

$$cL^2D \iint \left\{1 + \frac{1}{kD}(\ln A' + \gamma_e - \ln(\sin\gamma))\right\} \sin\gamma\, f(\mathbf{u}) f(\mathbf{u}') d\mathbf{u} d\mathbf{u}' \quad (1)$$

A' is given by Eq. (A1.2) in Appendix I, and γ_e = 0.577215665..... denotes the Euler's constant. $\mu^o(T)$ is the standard chemical potential of the particles at the temperature T in a solvent with chemical potential, μ_o; $c = N/\Omega$ is the number density; κ^{-1} is the Debye screening length; **u** and **u'** are the unit vectors along the two rods inclined at angle γ (Fig. 1); and k_B is the Boltzmann constant. In deriving the above equation, the interaction between two cylindrical rods at an inter-axial angle γ has been taken into account (cf. Equations (A.1) and (A.2)). The distribution function of rod orientation indicated by **u** is denoted by $f(\mathbf{u})$. Performing the integrals one eventually obtains the free energy in the isotropic phase

$$\frac{\Delta F_i}{Nk_BT} = \frac{\mu^0}{k_BT} - 1 + \ln c + \frac{\pi}{4} cL^2 D\left(1 + \frac{\ln A' + \gamma_e + \ln 2 - 0.5}{\kappa D}\right) \quad (2)$$

The second term in the parentheses on the right-hand side of Eq. (2) represents the effect of the electrostatic interaction on the free energy. The contribution can be interpreted as a change of the diameter of the rods by a factor

$$s = \frac{\ln A' + \gamma_e + \ln 2 - 0.5}{\kappa D} \quad (3)$$

Hence the effective diameter of the rod-like particle can be written as

$$D_{eff} = D(1 + s) \quad (4)$$

and the effective excluded volume

$$b_{eff} = \frac{\pi}{4} L^2 D_{eff} \quad (5)$$

We can write the free energy in the isotropic phase as

$$\frac{\Delta F_1}{Nk_BT}=\frac{\mu^o}{k_BT}-1+\ln c+b_{eff}c \tag{6}$$

In the anisotropic phase we have,

$$\frac{\Delta F_a}{Nk_BT}=\frac{\mu^0}{k_BT}-1+\ln c+\sigma_1+b_{eff}c(\rho+h\eta) \tag{7}$$

where, $\sigma_1(f)=\langle\ln(4\pi f(\mathbf{u}))\rangle_a=\int f(\mathbf{u})[\ln(4\pi f(\mathbf{u}))]d\mathbf{u}$

$$\rho(f)=\frac{4}{\pi}\langle\langle\sin\gamma\rangle\rangle_a \quad =\frac{4}{\pi}\int f(\mathbf{u})f(\mathbf{u}')\sin\gamma d\mathbf{u}d\mathbf{u}'$$

$$\eta(f)=\frac{4}{\pi}\langle\langle-\sin\gamma\ln(\sin\gamma)\rangle\rangle_a-\left(\ln 2-\frac{1}{2}\right)\rho(f) \tag{8}$$

In Eq. (7) and (8) the $<\ldots>_a$ suggests that the averaging has been done for the anisotropic or nematic phase. The twist parameter h is the ratio of the Debye length κ^{-1} and the effective diameter D_{eff}, i.e.,

$$h=\frac{1}{\kappa D_{eff}} \tag{9}$$

Using Equation (3) and results from Appendix I, it is easy to see that the expression for h has a negative logarithmic term, e.g., -ln κ, in the denominator of Eq. (9). This diverges to infinity as $\kappa\to 0$, i.e., as the solution becomes increasingly devoid of small electrolytes. This means that $h\to 0$, i.e., the hard rod problem. In the isotropic state, ρ = 1 and η = 0. Concentrations of the coexisting phases are found by applying the coexisting conditions, i.e., the equality of the osmotic pressure (π_1) and the chemical potential (μ') in the two coexisting phases, i.e.,

$$\frac{\pi_1}{k_BT}=k_BTc\left[1+b_{eff}c(\rho+h\eta)\right] \tag{10}$$

$$\mu'=\mu^0+k_BT\left(\ln c+\sigma_1+2b_{eff}c(\rho+h\eta)\right) \tag{11}$$

In order to find the coexisting concentrations c_i and c_a in the isotropic and anisotropic phases, one has to solve the coexisting equations,

$$c_i\{1 + c_i\} = c_a\{1 + c_a[\rho_a + h\eta_a]\} \tag{12}$$

$$\ln c_i + 2c_i = \ln c_a + \sigma_1 + 2c_a[\rho_a + h\eta_a] \tag{13}$$

The Onsager theory is known to become exact in the limit of axial ratio L/D $\rightarrow \infty$ [4], and all the virial coefficients higher than the second tend towards zero in this case. For lower axial ratios, the third and the higher virial coefficients become non-zero. In attempting to apply the Onsager theory to a natural protein polymer such as F-actin, one needs to modify the theory to include the electrostatic repulsion between the double layers. This has the effect of lowering the axial ratio as a result of rod diameter enhancement, as well as skewing the interacting rod axes as measured by a twist parameter $h = (kD_{eff})^{-1}$. The twisting effect serves to destabilize the liquid crystal phase, shifting it to a higher concentration. However, in practice, rod thickening effect seems to dominate the twisting effect.

Stability Criterion for the Isotropic Phase : *Repulsion plus Attraction* — The above treatment of isotropic-nematic phase separation takes into account steric and non-steric repulsive interactions only. However, it is clear that attractive interactions are ubiquitous; hence the above model based on repulsive interactions only is in a sense inadequate. In this section we summarize Odijk's arguments showing that the isotropic phase becomes unstable with respect to phase separation, gelation or aggregation as the third virial coefficient becomes large as a result of long-range attraction. It has already been noted that the effect of the electrostatic repulsion will be equivalent to an increase of the effective diameter (D_{eff}), which will be dependent on the thickness of the electric double layer and thus on the ionic strength. Two test polyions are prevented from approaching each other closer than D_{eff} in view of the repulsive electrostatic force. This argument is legitimate even when the macromolecules are enclosed in the confined oriented space,

$$\gamma \leq p^{-1} \equiv \frac{\xi}{L} \quad (\xi \text{ is the decay length}).$$

Configurations that are almost parallel give the largest contributions to the virial coefficients. The second virial coefficient may be written as

$$B = B_{el} + B_A \tag{14}$$

where electrostatic contribution can be represented as [12],

$$B_{el} \approx \frac{\pi}{4} L^2 D_{eff} \tag{15}$$

Using the definitions described by Eq. (3) and (4), the attractive contribution to the second virial coefficient is given by

$$B_A = -\frac{1}{32\pi^2}\iiint d\mathbf{u}d\mathbf{u}'d\Delta\mathbf{R}\,\Phi_A(\Delta\mathbf{R},\mathbf{u},\mathbf{u}') \tag{16}$$

where we have used $f(\mathbf{u}) = f(\mathbf{u}') = 1/4\pi$, as is appropriate for the isotropic phase. Here, as before, **u** and **u**' are the orientational unit vectors along the two test polyion long axes, and $\Delta\mathbf{R}$ is the vector distance between their centers of mass (Fig. 1). $F_A = \exp(w_A/k_BT) - 1$, is the Mayer function (w_A has been taken

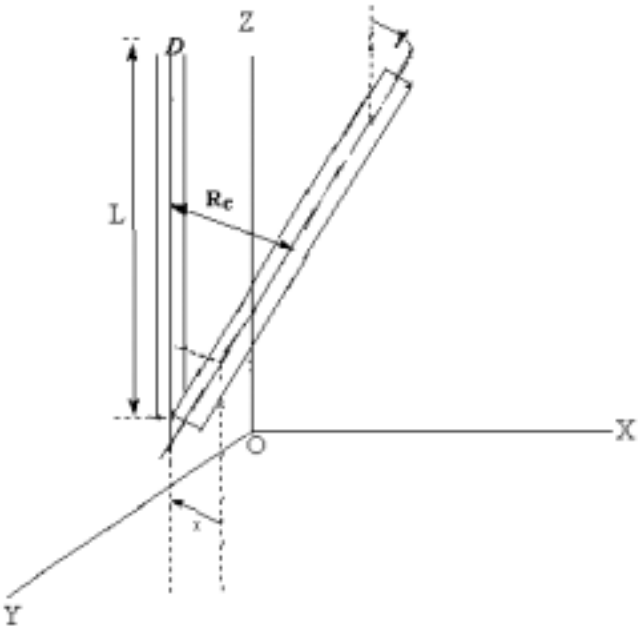

Fig. 1. The configuration of two rods of equal length *(L)* and diameter *(D)*, skewed at an an gle γ. The distance between the centerlines is denoted by x; R_c is the vector distance between the centers of mass of the two rods.

from Eq. (A2.3)). Since parallel configurations are the most heavily weighted ones, each of the two integrations over orientational variables gives $2\pi/p$. Then, using cylindrical polar coordinates one writes Eq. (16) as

$$B_A \approx \frac{1}{8p^2}\int_0^{2\pi} d\phi \int_{-L}^{L} d\Delta z \int_{D_{eff}}^{\infty} (1 - e^{-W_A/k_BT})x\,dx = -\frac{\pi L\xi^2 J\left(\frac{\mu}{\alpha}\right)}{2p^2} \tag{17}$$

$$\text{with } J\left(\frac{\mu}{\alpha}\right) \equiv \int_{D_{eff}/\xi}^{\infty} dX\, X\left[\mu^{-1} e^{X+\mu e^{-X}} - \mu^{-1} e^{-X} - 1\right] \tag{18}$$

$$\text{and } \mu = LH/\xi\ ; \quad \alpha = \exp(D_{eff}/\xi);\ \text{and } X = x/\xi. \tag{19}$$

Odijk [12] has shown that

$$J(z) = I(z) - e^z / z + 1 / z + 1 \tag{20}$$

$$\text{with } z = \mu/\alpha, \text{ and where } I(z) = \sum_{n=1}^{\infty} \frac{z^n}{n!\, n} \tag{21}$$

$$\text{Also, } J(z) \sim e^z / z^2 \qquad (z \geq 1) \tag{21a}$$

Hence the relative attractive contribution to the second virial coefficient is

$$\eta_2 = -\frac{B_A}{B_{el,0}} \approx \frac{2\xi^4 J(\mu/\alpha)}{L^3 D_{eff}}. \tag{22}$$

Unlike the second virial coefficient, the third virial coefficient is not separable into purely electrostatic repulsive and attractive terms [12, 16]

$$C = C_{el} + C_A + C_{el,A} \tag{23}$$

The first two terms represent purely the three body electrostatic repulsion and attractive terms. The third term, $C_{el,A}$ is the mutual interaction term between electrostatic repulsion and attraction among three rods. Odijk [12] expresses them as

$$C_{el} \approx \frac{4 D_{eff} B_{el}^2}{L} \quad ; \quad C_{el,A} \approx B_A B_{el} \quad ; \quad C_A \approx B_A^2 e^{\mu/\alpha}$$

The relative attractive contribution to C can be expressed as

$$\eta_3 \equiv \frac{\left|C_A + C_{el,A}\right|}{C_{el}} = \frac{L}{4 D_{eff}} \left(\eta_2^2 e^{\frac{\mu}{\alpha}} + \eta_2 \right) \tag{24}$$

The influence of attractive forces on the third virial coefficient is much greater than on the second virial one, especially when $z = \mu/\alpha \geq 1$. Hence under certain conditions the third virial coefficient may be negative whereas the second remains positive. There is a distinct possibility of the solution becoming unstable. If the

osmotic pressure for an isotropic solution is given by

$$\pi_1 = k_B T\left(1 + Bc + Cc^2 + \ldots\ldots\right) \tag{25}$$

where c is the number density, we require

$$\frac{\partial \pi_1}{\partial c} \geq 0 \tag{26}$$

for the solution to remain stable (the sign of equality indicating the onset of instability). Now neglecting virial coefficients higher than the third, and using

$$B = (1-\eta_2)B_{el} \quad ; \quad C = (1-\eta_3)C_{el} \tag{27}$$

on the basis of Eq. (22) and (24), we thus have the criterion for the onset of instability

$$Y \equiv \frac{D}{L} + \left(\frac{2D_{eff}}{D}\right)\phi_1(1-\eta_2) + \frac{3}{2}\left(\frac{2D_{eff}}{D}\right)^3 \phi_1^2(1-\eta_3) \geq 0 \tag{28}$$

where $\phi_1 = \pi(D/2)^2 Lc$ is the macromolecular volume fraction.

Equation (28) agrees with that given in [12], except for the appearance of η_2, which Odijk neglected apparently to ensure a positive B. The sign of equality applies to the onset of instability. The "greater than" sign indicates the stability of the isotropic phase. It is applicable equally to phase separation, gelation or aggregation, because all of these are governed by long-range attraction.

RESULTS

i) *When attraction is not considered*

Along the length of the F-actin chain, there are four electronic charges per nm [15]. Then the surface charge density is

$$\sigma = \frac{4e}{\pi DL} = 0.026 \ \text{Cm}^{-2},$$

assuming 4 nm to be the radius of the actin cylinder and that the cylinder is so long that end effects can be neglected. However proteins have ionizable surface sites that are almost fully dissociated since the pK values of constituent amino acids typically differ much from 7, the pH of the solution in the case of F-actin. We know that the relation between the surface charge density σ and the surface potential ψ can be conveyed by Grahame equation [16]. For the case of a mixed

$KCl+MgCl_2$ electrolyte, the Grahame equation can be written as [16]

$$\sigma = 0.117 \sinh\left(\frac{\psi}{51.4}\right)\left\{[KCl]+[MgCl_2]\left(2+\exp\left(-\frac{\psi}{25.7}\right)\right)\right\}^{\frac{1}{2}} \tag{29}$$

where the concentrations in bulk $[KCl] = \left[K^+\right]_\infty$ and $[MgCl_2] = \left[Mg^{2+}\right]_\infty$ are taken in units of moles/liter, ψ in mV, and σ in C/m^2. Equation (17) allows us to calculate ψ once σ is known. In the case of F-actin, using σ = 0.026 C m^{-2}, the surface potential of F-actin can be found from Grahame equation (17) as Ψ = 33.0079 mV. In that weak potential limit the linear charge density from equation (15) of F-actin is $\nu_h = 1.6256 \times 10^{-8}$ C/m.

Using the Onsager model modified by Stroobant et al. the results, given in Table 1, pertain to an F-actin system where I-N phase separation is known to occur [14]. The filaments, 2 mm long on average, are immersed in a solution of concentration 15 mg/ml with excess 1-1 (100 mM of KCl) and 2-1 (2 mM of $MgCl_2$) electrolytes. The Debye length is then $\lambda = \kappa^{-1} = 0.9429$ nm. Taking 4 nm to be the radius of the actin cylinder, D_{eff} has been found to be 10.12 nm, on the basis of Eq. (4) (using the full series for $K_1(\kappa D/2)$ from MATHEMATICA 4.1) and (A1.2). From Equation (9) one then obtains h = 0.0932.

TABLE 1

Convergence of the Concentrations, Order Parameter S, and Orientation-Dependent Free Energy Terms of the Coexisting Isotropic (c_i) and Anisotropic Phase (c_a), Osmotic Pressure, Chemical Potential, for the F-actin system, using the expansion of $\sin\gamma$ in Legendre Polynomials $P_{2n}(\cos\gamma)$, Truncated at n = 7; $S = < P_{2n}(\cos\theta) >$.

c_i	c_a	S	σ_1	ρ	η	π_1	μ
3.52	4.48	0.809	1.70	0.54	0.28	15.89	8.29

c_i and c_a are in unit of 1/DL^2; π_1 and μ are in unit of k_BT.

ii) *When attraction is considered*

Including attractive interaction is trickier since denser parallel alignment is disfavored in the repulsive case while being favored in the attractive case. This implies that higher virial coefficients may exceed the second in this case, complicating the calculation very much. For the F-actin system, long-range attraction is obviously important.

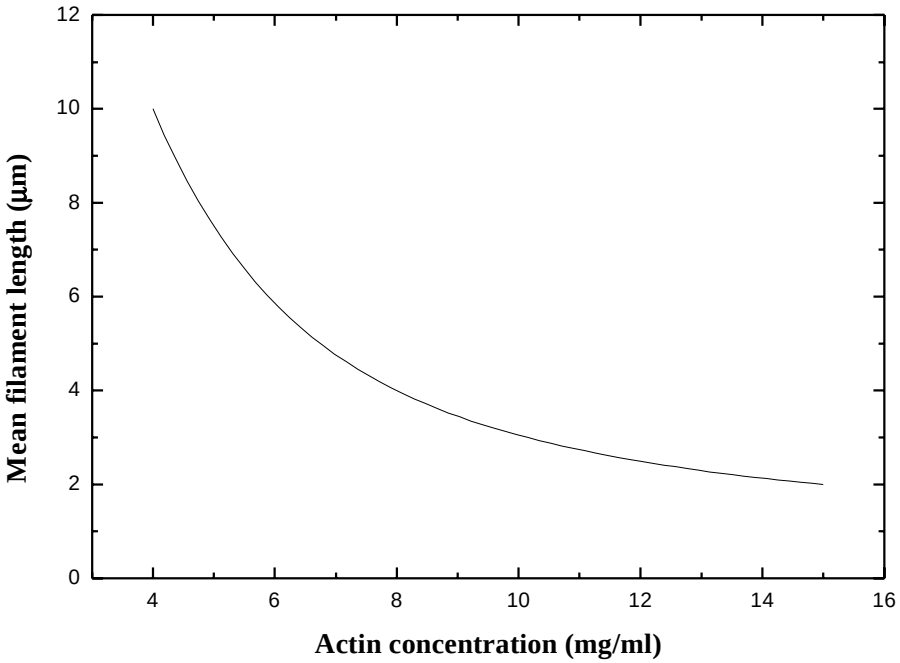

Fig. 2. I-N phase boundary of F-actin has been constructed with data from references, [14] and [20].

We cite an example of application of Eq. (28) to I-N phase diagram (Fig. 2) of F-actin depicting average filament length in microns versus actin concentration in mg/ml. In Fig. 3 left hand side of Eq. (28) has been plotted as a function of polymer length L for $H = 0.005$. Since H does not depend on L (cf. Eq. (25)), it is of some interest then to see how Y, i.e., the left hand side of Eq. (28) behaves as a function of L (Fig. 3). It is clear that Y does not take on a negative value for any value of $z = \mu/\alpha$ in the practically realizable L range of 1 to 70 μm, so long as $z << 1$, becoming insensitive to L variation in the range $\sim$ 20 – 70 μm. However, for 2 μm long filaments which produce a phase separation into isotropic and nematic phases at a concentration of 15 mg/ml [14], an upper bound for H can be obtained from Eq. (28) at $z = 12.45$, which corresponds to $H = 0.1825$. This is where an isotropic-nematic phase separation (tactoid formation followed by phase separation) occurs [14]. Using Eq. (25), $m_1 \sim 2.5$ is obtained, since $h_1 \sim 20$ is established experimentally [12]. The following parameters pertaining to F-actin have been used for the construction of Table II : the bare diameter $D = 8$ nm, the molar mass per unit contour length,

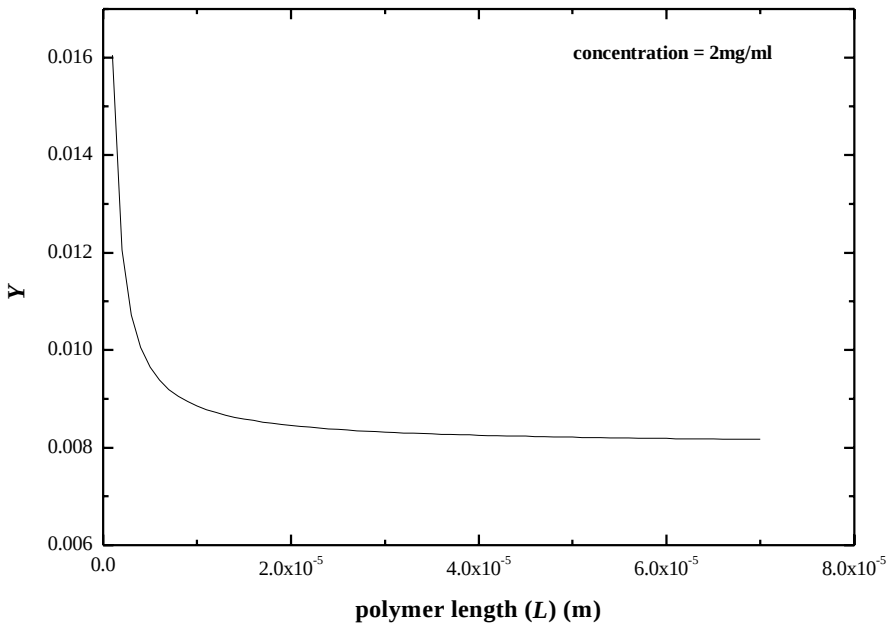

Fig. 3. Plot of left hand side of Eq. (28) as a function of polymer length (L) (in m). H = 0.005 has been used for this calculation.

M/L = 15.17 kg/mol nm [20], the Bjerrum length Q = 0.714 nm at room temperature, and charge spacing 0.25 nm per electron charge [2]. A 36 nm long (pitch) F-actin chain has 13 G-actin moieties, each having a mass of 42 kD. Table II shows critical H and h_3 (i.e., the H and η_3 at which Y becomes equal to zero) values for the onset of instability seen in F-actin solution, e.g., isotropic-nematic phase transition.

The variation of total interaction energy,

$$W = \frac{w_{el,P}}{k_B T} + \frac{w_{A,P}}{k_B T}$$

with centerline separation x (m) have been compared in Fig. 4, for F-actin solution with average filament length 2, 4 and 10 μm with electrolyte concentrations : 100 mM KCl and 2 mM $MgCl_2$. Table II gives the critical H values for the different filament lengths chosen above. For a somewhat higher concentration of electrolytes, e.g., 150 mM KCl and 10 mM $MgCl_2$, a hexagonal LC phase results leading to a six-fold increase in interaction [11].

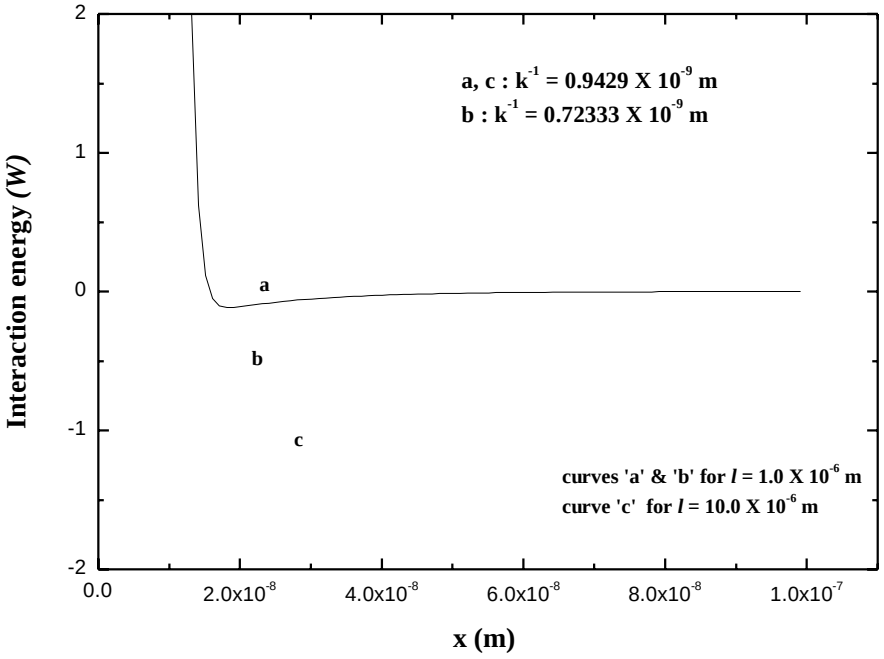

Fig. 4. Schematic diagram of interaction energy (W) versus inter-rod distance x (in m). The minimum responsible for isotropic-nematic phase transition for Debye length a, c : 0.9429 nm; with electrolyte concentration as 100 mM KCl and 2 mM $MgCl_2$ and for Debye length b : 0.72333 nm caused by the electrolyte concentration as 150 mM KCl and 10 mM $MgCl_2$.

TABLE 2

Critical H for isotropic to nematic phase transition in F-actin solution with Debye screening length λ = 0.9429 nm has been determined from Eq. (21), (21a) and (28) using MATHEMATICA 4.1; with salt concentration KCl : 100 mM and $MgCl_2$: 2 mM and effective diameter of the filament is D_{eff} = 10.12 nm.

n_s (M)	ρ(mg/ml)	$l(\mu m)$	ϕ_1	η_3	H
0.106	4.0	10.0	0.007984	14.4778	0.04334
0.106	8.0	4.0	0.015968	7.82294	0.09438
0.106	15.0	2.0	0.02994	4.66228	0.166907

DISCUSSION

The use of the second virial approximation is tenable for the approaches of Onsager

and Stroobant et al. where predominantly repulsive interactions are involved. At present no reliable measurement of order parameter in the F-actin system is available to be compared to our estimate. Real systems such as F-actin, however, admit of attractive interactions also, particularly at higher ionic strength. The third and higher virials then may become comparable to or greater than the second virial, leading to a breakdown of the second virial approximation. Under this condition, an aggregation to a hexagonal phase [13] or bundling (paracrystals) [15] is a distinct possibility.

The attribution of the long-range attraction to just hydrophobic interaction is somewhat questionable since Van der Waals forces also may have a contribution. However, we have tried to keep the mathematics tractable. Also, at low salt concentration, hydrophobic interaction should have the upper hand [12]. The coordinates from the I-N phase diagram (Fig. 2) appear to fit Eq. (28) with a single value of H.

As pointed out in section I, the prediction of the phenomenological Landau-deGennes approach is that the I-N transition is weakly first-order. Mean-field theory does not describe it fully, and fluctuations do play an important role [5]. Since actin filaments are each a few microns long, the correlation length near the I-N phase boundary is likely to be a few hundred microns, and a physical gel is actually obtained [13]. The Onsager and Stroobant theories deal with phase separation since only repulsive interaction is involved. Attractive interaction may cause a pre-transitional ordering of the filaments, inducing a continuous transition. A continuous I-N transition cannot definitely be ruled out [5, 14].

CONCLUSION

We conclude that in I-N phase separation the attractive part of the second virial coefficient is less than its electrostatic repulsive counterpart in magnitude, keeping the net second virial co-efficient positive. However, the attractive part of the third virial coefficient is significantly larger than its electrostatic repulsive counterpart so that the net third virial co-efficient is negative. As the present study suggests, the I-N phase boundary may be reconciled with a model showing an attractive term dependent on few parameters. Refinements like including Van der Waals contribution may be attempted in future.

APPENDIX I : INTERACTION BETWEEN CHARGED RODS

Since the second virial coefficient is determined by the contact between the outer parts of the double layers, one can approximate the interaction between the line

charges, at the shortest distance x and mutual angle γ in the Debye-Hückel limit by [17],

$$\frac{w^{el}}{k_B T} = \frac{2\pi \nu_{eff}^2 Q e^{-kx}}{\kappa \sin\gamma} = \frac{A' e^{-\kappa(x-D)}}{\sin\gamma} \tag{A1.1}$$

where $A' \equiv \dfrac{2\pi \nu_{eff}^2 Q e^{-\kappa D}}{\kappa}$ (A1.2)

and the Bjerrum length, $Q = e^2/4\pi\varepsilon_0\varepsilon k_B T$, ε being the dielectric permittivity.

For low surface potential, Equation (A1.1) holds at all distances $x > D/2$. In that weak potential limit, we have

$$\nu_{eff} = \frac{2\pi\sigma}{\kappa K_1\left(\dfrac{\kappa D}{2}\right)} \tag{A1.3}$$

where σ is the surface charge per unit area of the cylinder, given by $\nu/2\pi$, ν being the actual linear charge density, and K_1 is the first order modified Bessel function of second kind. For thin ($\kappa D > 1$) double layer, one obtains the leading term $A' \sim 8\nu^2 Q / D\kappa^2$. Thick ($\kappa D < 1$) double layers give $A' \sim 2\pi\nu^2 Q\kappa^{-1}$ on the basis of a series expansion [18].

Now, the total cluster integral

$$\beta(\gamma) = \beta_s(\gamma) + \beta_{ns}(\gamma)$$

has a steric part given by $\beta_s(\gamma) = -2L^2 D \sin\gamma$ and a non-steric part given by

$$\beta_{ns} = 2L^2 \sin\gamma \int_D^\infty (e^{-w_{el}/k_B T} - 1)dx$$

$$= -2\kappa^{-1} L^2 \sin\gamma[\ln(A'/\sin\gamma) + \gamma_e + E_1(A'/\sin\gamma)]\,. \tag{A1.4}$$

$\gamma_e = 0.577215...$ is the Euler constant, and E_1 is the exponential integral [15]. For $A' > 2$, the argument of E_1 is larger than 2, in which range the exponential integral may be neglected. Now the mutual interaction energy between two parallel rods separated by inter-axial distance Δz is [12, 19],

$$w_{el,P} = \frac{\left(A'e^{\kappa D}\right)L\left(1 - \frac{|\Delta z|}{L}\right)e^{-\kappa x}}{D_{eff}}; \qquad -L \le \Delta z \le L,\ \gamma \le \frac{D_{eff}}{L} \tag{A1.5}$$

D_{eff} is the effective diameter which scales approximately as the Debye length $\lambda = \kappa^{-1}$. Δz is the distance between the centers of mass of the two rod-like polyions along the z-axis. The electrostatic energy is purely exponential in separation and decrease with increasing distance between the centers of mass of the two rods.

APPENDIX II : ATTRACTIVE INTERACTION BETWEEN TWO RODS

The long-range attraction between hydrophobic surfaces in polyions has been studied by colloid scientists [12]. It is asserted to be weak but of long-range, with potentially important contribution to phase transitions, etc. A brief quantitative description of this interaction is given below.

The area of interaction for two crossed cylinders in the limit $D/2 << \xi$, is independent of cylinder radius $D/2$ and scales as ξ^2 if one assumes that a polyion perturbs the surrounding water over a distance of order ξ (a decay length of about 14 nm) by its mere presence. Furthermore, it is conceivable that the influence of the electric double layer on the attraction is altered by the fact that $D/2$ is no longer much greater than ξ so this might introduce a power law κ^{-m_1} with $m_1 \neq 1$, (κ^{-1} is the Debye screening length). For cylinders skewed at an angle γ, the area of interaction is inversely proportional to sin γ (Fig.1). Therefore, for a monodisperse suspension of rod-like macromolecules each of length L and diameter D, the attractive interaction between the cylinders is [12]

$$\frac{w_A}{k_B T} = -\frac{He^{-x/\xi}}{\sin\gamma} = -\frac{H'e^{-(x-D)/\xi}}{\sin\gamma}; \qquad \gamma \ge p^{-1} \equiv \frac{\xi}{L} < 1 \tag{A2.1}$$

$$\text{with} \quad H = \frac{h_1}{\kappa^{m_1}}(a+\xi)\xi^{-(m_1+1)}\exp\left(\frac{D}{\xi}\right) \tag{A2.2}$$

$$H' = He^{-D/\xi}$$

where h_1, a coupling constant, has been found to be about 20. Eq. (A2.1) breaks down when the polyions are almost parallel. Then we have

$$\frac{w_A}{k_B T} = -pH\left(1 - \frac{|\Delta z|}{L}\right)\exp\left(-\frac{x}{\xi}\right) \qquad \gamma \le p^{-1} \equiv \frac{\xi}{L}; -L \le \Delta z \le L \qquad \text{(A2.3)}$$

One of the rods is placed along the z-axis of a cartesian co-ordinate system.

REFERENCES

1. B. Alberts, D. Bray, J. Lewis, M. Raff, K. Roberts and J. D. Watson, Molecular Biology of the Cell, Garland, New York (1998).
2. A. Suzuki, T. Maeda and T. Ito, Biophys. J. 59, 25 (1991).
3. J. D. Bernal and I. Fankuchen, Nature 139, 923 (1937).
4. L. Onsager, Ann. N. Y. Acad. Sci. 51, 627 (1949).
5. P. G. deGennes and J. Prost, "The Physics of Liquid Crystals", Clarendon, Oxford (1993)
6. M. Doi and S. F. Edwards, "The Theory of Polymer Dynamics", Clarendon, Oxford (1986).
7. A. Stroobants, H. N. M. Lekkerkerker and T. Odijk, Macromolecules 19, 2232 (1986).
8. A. Donald, A. Windle and S. Hanna, "Liquid Crystalline Polymers", 2nd ed., Cambridge University Press, Cambridge (2006);
9. C. Tanford, The Hydrophobic Effect, Wiley, New York (1980).
10. J. L. Parker, D. L. Cho, P. M. Claesson, J. Phys. Chem. 93, 6121 (1989); H. K. Christenson, P. M. Claesson, J. Berg and P. C. Herder, J. Phys. Chem. 93, 1472 (1989).
11. E. J. W. Verwey and J. TH. G. Overbeek, Theory of the Stability of Lyopho bic Colloids, Dover Publications, Inc., Mineola, New York (1999).
12. T. Odijk, Macromolecules 27, 4998 (1994).
13. P. Das, J. Roy, N. Chakrabarti and S. Basu, J. Chem. Phys. 116, 9028 (2002).
14. J. Viamontes, P. W. Oakes and J. X. Tang, Phys. Rev. Lett. 97, 118103 (2006).
15. J. X. Tang and P. A. Janmey, J. Biol. Chem. 27, 8556 (1996).
16. P. V. Schoot and T. Odijk, J. Chem. Phys. 97, 515 (1992).
17. S. L. Brenner and V. A. Parsegian, Biophys. J. 14, 327 (1974); M. Fixman and J. Skolnick, Macromolecules 11, 863 (1978).

18. M. Abramowitz and I. A. Stegun, Handbook of Mathematical Functions, National Bureau of Standards, Washington (1964).
19. G. J. Vroege and H. N. W. Lekkerkerker, Rep. Prog. Phys. 55, 1241 (1992).
20. C. M. Coppin and P. C. Leavis, Biophys. J. 63, 794 (1992).